Available online at www.sciencedirect.com
ScienceDirect
Ultrasonics 44 (2006) e801–e806
Ultrasonics
www.elsevier.com/locate/ultras

Differential geometry of ray surfaces in anisotropic solids and its contribution to NDE: Modelling and experiment

Hanuš Seiner [a,b], Michal Landa [b,*]

[a] CTU, Faculty of Nuclear Sciences and Physical Engineering, Department of Materials, Trojanova 13, 120 00 Prague 2, Czech Republic
[b] Institute of Thermomechanics, Czech Academy of Sciences, Dolejškova 5, 182 00 Prague 8, Czech Republic

Available online 9 June 2006

Abstract

Point-source/point-receiver techniques are one of the most widely used methods for nondestructive evaluation of anisotropic materials. The group velocities resulting from these techniques must be, for further inverse evaluation of elastic coefficients, geometrically converted into corresponding phase velocities. On the other hand, the phase velocities can be determined from a material's response to a line source. But, due to the anisotropy, the short line sources generated by cylindrical lenses are insufficient for reliable determination of the phase velocity. In this paper, a long line source is approximated by a set of linearly arranged point sources. As it follows from the differential geometry of ray surfaces, information obtained from such set of sources is sufficient for determination of phase velocities of both the quasi-transverse and the quasi-longitudinal modes of propagation. Moreover, this approach can be generalized for any arbitrary set of point sources only by employing a proper time-base transformation. The applicability of the presented approaches is illustrated on transversely isotropic and tetragonal fibrous composite materials.

Keywords: Anisotropic materials; Composites; Differential geometry; NDE; Automation

1. Introduction

In the last 20 years, the point-source/point-receiver (PS/PR) techniques for nondestructive ultrasonic evaluation of anisotropic materials have been developed and validated for a wide range of materials [1–4], primarily for fibreous composites [5–10]. PS/PR techniques usually result in an extensive set of group velocities of elastic wave propagation in various material directions. From this data the elastic coefficients are inversely determined. For a stable and reliable inversion, the group velocities must first be geometrically converted into phase velocities (e.g. [3]). This can induce systematical errors, especially in nondiagonal elastic coefficients [11]. Moreover, the geometrical conversion into the phase velocities generally complicates the entire procedure's automation, because the reliability of the chosen fitting function and the converted phase velocities must be verified for each particular inversion.

This paper presents some possibilities of direct experimental determination of phase velocities in certain directions. Signals from point-like sources are still detected by a point-like detector, but the geometrical arrangement of the source array is beneficially utilized, and exploits consistently the differential geometry of ray surfaces. This paper deals with a set of point-like sources arranged in a line, called here, for simplicity, *a linear array*. In the last section only, a possible generalization to a circular array is presented. Determination of the phase velocity is the main objective of this paper; the experimental results and numerical simulations are presented only to illustrate the method's applicability on particular examples. To mention briefly the experimental setup – the laser point-like source (General Photonics Corporation Nd:YAG laser, dominant wavelength 1064 nm, optical path width 12 ns) was used to scan a free surface of the composite specimen. The acoustic signals from local vaporization were detected by

* Corresponding author. Fax: +420 286 584 695.
E-mail address: ml@it.cas.cz (M. Landa).

0041-624X/$ - see front matter © 2006 Elsevier B.V. All rights reserved.
doi:10.1016/j.ultras.2006.05.139

a miniature piezoelectric PIN-ducer VP-1093-A50, situated on the same free surface, and recorded by a Nicolet(12 bits, 100 MS/s) ACCURA 100 digital oscilloscope. For further details in instrumentation, see [8–10,12].

2. Wave arrivals from a linear array of independent point-like sources

Let us consider a free surface of an anisotropic material, and let this surface be parallel to one of the material's symmetry planes. The cartesian coordinates $[x_1, x_2, x_3]$ are introduced such that the x_2-axis is normal to the free surface, as outlined in Fig. 1. The point-like detector is situated at the origin of this cartesian system. Let the angle β denote a general direction in the x_1x_3-plane, and let us consider an infinite linear array of point-like sources in the distance d from the origin forming the angle β with the x_3-axis. The positions of particular sources of this array are represented by one spatial coordinate y, or, equivalently, by one angular coordinate α, with $y = 0$ for $\alpha = 0$ (see Fig. 1). The distance between two neighboring sources is denoted Δy and considered as constant. For $\Delta y \ll d$, the signals obtained successively from all sources can be treated as a continuous wave field in the $[y, t]$-space.

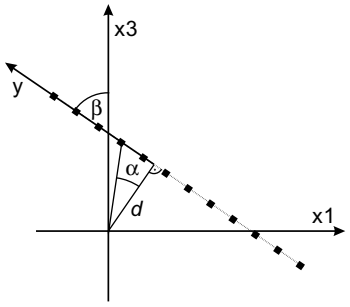

Fig. 1. A linear array of point-like sources represented by a spatial coordinate y, or, alternatively, by one angular coordinate $\alpha = 0$. The detector is situated in the origin, and d denotes its distance from the array.

Let us first focus on the fastest quasi-longitudinal (qL) mode. The time of flight (TOF) of the qL-pulse from the source to the detector is given by the group velocity v_G in direction $(\alpha(y) + \beta)$. Because the distance between the actual source and the detector can be expressed as $d/\cos\alpha$, the TOFs satisfy the equation

$$\mathrm{TOF}(y) = \frac{d}{\cos(\alpha(y))v_G(\alpha(y) + \beta)}. \tag{1}$$

For an isotropic material, the resulting function TOF(y) should have a minimum in $y = 0$, and should be symmetric about this point. Due to directional dispersion in the anisotropic material, the minimal TOF deviates from the symmetric position as can be seen on examples in Fig. 2, where the $[y, t]$-fields are compared to exactly evaluated wavefront arrivals.

The extremal condition on TOF(y) is

$$\begin{aligned} 0 = \tfrac{\mathrm{dTOF}(y)}{\mathrm{d}y} &= \frac{\mathrm{d}}{\mathrm{d}\alpha}\left(\frac{d}{\cos(\alpha)v_G(\alpha+\beta)}\right)\cdot\frac{\mathrm{d}\alpha}{\mathrm{d}y} \\ \Rightarrow \frac{\mathrm{d}}{\mathrm{d}\alpha}&(\cos(\alpha)v_G(\alpha+\beta)) = 0, \end{aligned} \tag{2}$$

for obviously

$$\cos(\alpha) \neq 0, \quad v_G(\alpha+\beta) \neq 0, \quad \text{and} \quad \frac{\mathrm{d}\alpha}{\mathrm{d}y} \neq 0. \tag{3}$$

For an infinite length of the array, (2) has always a solution. When considering a real array of a finite length, we must require the absolute values of angles α^{end} corresponding endpoints of the array to be greater than the maximal possible angular difference between the group and phase velocity in the evaluated material. For fibreous composites [5–10], our choice $|\alpha^{\mathrm{end}}| > 50°$ appears to be sufficient.

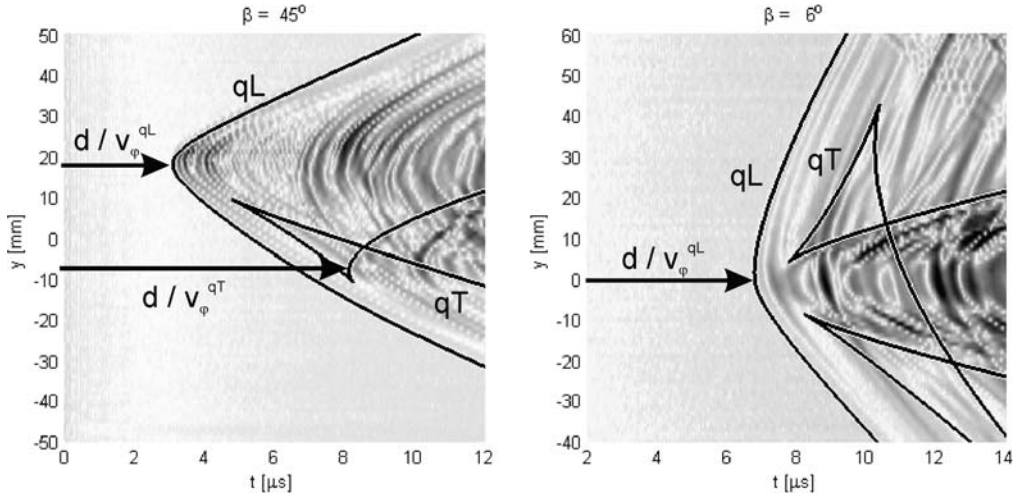

Fig. 2. Examples of $[y, t]$ fields experimentally obtained from two linear arrays of point-like sources forming the angles $\beta = 6°$ and $\beta = 45°$ with the x_3-axis. The tested material was a 8 mm thick plate of a unidirectional CFRP composite with the fiber direction parallel to the x_3-axis. The array was situated in the distance $d = 20$ mm, and consisted of 101 point-like sources spaced by $\Delta y = 1$ mm, between $y = -50$ mm and $y = 50$ mm. For comparison, thick lines denote the arrivals of particular wavefronts evaluated for known elastic coefficients.

Let α_0 denote the angle for which the minimum reached. Recasting the condition (2) into

$$\left.\frac{\mathrm{d}v_{\mathrm{G}}(\alpha+\beta)}{\mathrm{d}\alpha}\right|_{\alpha=\alpha_0} = v_{\mathrm{G}}(\alpha_0+\beta)\cdot\tan\alpha_0, \tag{4}$$

we realize that the normal to the ray surface in point $(\alpha_0+\beta)$ has the direction given by β. In the other words, the minimal TOF determines the phase velocity v_φ in the chosen direction β [3,5]

$$\mathrm{TOF}(\alpha_0) = \frac{d}{v_{\mathrm{G}}(\alpha_0+\beta)\cdot\cos\alpha_0} = \frac{d}{v_\varphi(\beta)}, \tag{5}$$

as denoted by arrows in Fig. 2. Moreover, the extremal angle α_0 determines the direction of the corresponding group velocity, satisfying the well-known geometrical relation $v_\varphi(\beta) = v_{\mathrm{G}}(\alpha_0+\beta)\cdot\cos\alpha_0$ [13–15].

It must be pointed out that the condition (2) is always satisfied in only one point of the ray surface. In the case of the quasi-transverse (qT) mode, where singular cuspidal features may appear, this point does not necessarily represent the first mode's arrival on the detector. It can be a local minimum on one of the pure convex/concave branches of this mode, while other branches can be faster. For $\beta = 45°$, in Fig. 1, the minimum on the qT-curve is easily detectable, and the corresponding phase velocity can be determined. However, for $\beta = 6°$, the minimum is situated on a low-energy branch of the qT-curve, and its reliable determination is, thus, close to impossible.

3. Superposition approach

Although the extremal TOF from a linear array of sources directly determines the phase velocity in chosen direction, further simplification can be discussed. Due to the considered linearity of observed waves, the superposition of signals from a dense linear array are expected to

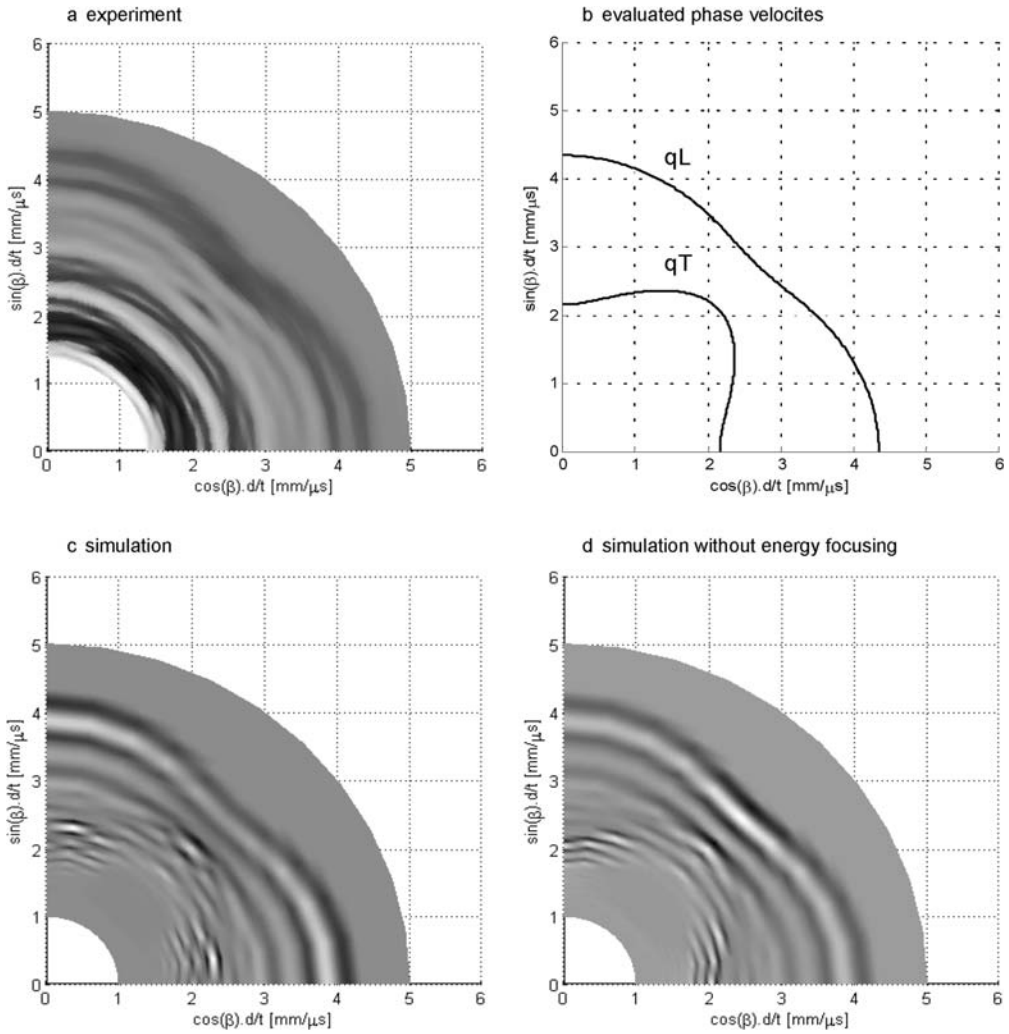

Fig. 3. Experimental verification of the superposition principle (a), compared to simulations for the qL and qT modes with and without energy focusing involved (c, d). Solid lines in (b) show the exact normal surfaces. The tested material was a 7.5 mm thick plate of a GFRP tetragonal composite with the fibres parallel to axes x_1 and x_3. The resultant signals were superposed from 80 mm long arrays, forming the angles $\beta = 0°, 9°, \ldots, 90°$ with the x_3-axis. Each array consisted od 81 point-like sources between $y = -40$ mm and $y = 40$ mm (spatial resolution $\Delta y = 1$ mm), and was situated in the distance $d = 30$ mm from the detector.

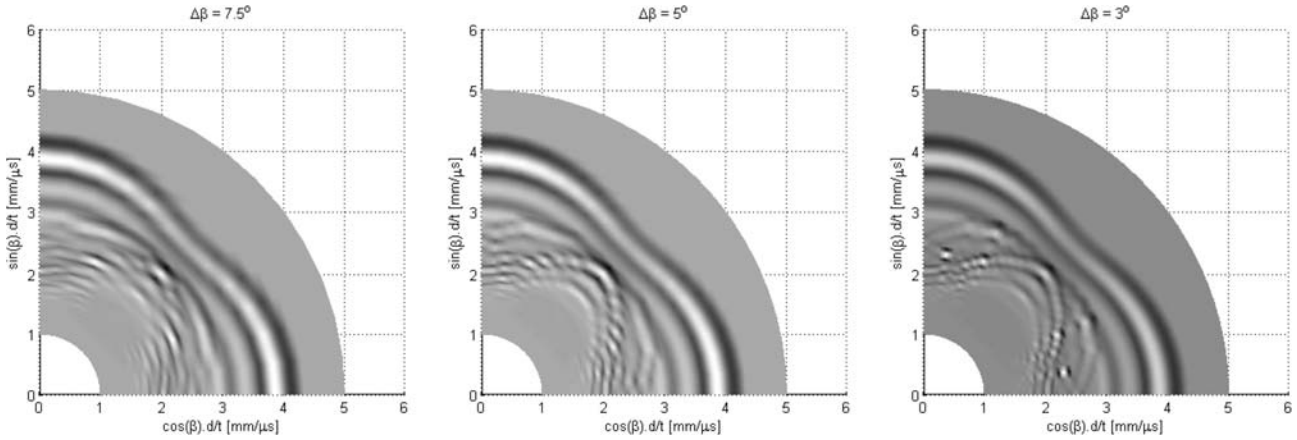

Fig. 4. Effect of the angular step in angle β on resultant superposed field for the same material and the same geometrical configuration as in Fig. 3.

be similar to a response to one long line source, which is a planar wave travelling at a phase velocity. For such response, the whole problem is reduced to a 1D detection of wave-front arrivals. This approach brings additional constraints on the source-receiver geometrical configuration. The length L and minimal distance between the source line and the receiver are required to satisfy the condition of near-field of the finite line source: $d/L < 1$ (suppression of influence of the line edges to the resulting wavefield). The length L of the array must also be long enough as to generate fundamental wave with maximal angle differences between the group velocity and related phase velocity. The incremental distance between nearby source points of the array is supposed less than wavelength of the source function. In our case, the selected increment length is 1 mm, and the frequency band of acquisition is 2 MHz, hence corresponding minimal wavelength is 2.5 mm for maximal expected wave velocity 5 mm/μs.

Both extensive experiments and numerical simulations were performed to explore this possibility. A tetragonal GFRP composite was tested using a set of linear arrays, corresponding to angles $\beta = 0°, 9°, \ldots, 90°$. A polar plot of superposed signals for the distance $d = 30$ mm, the array of total length 80 mm spaced by $\Delta y = 1$ mm, is shown in Fig. 3a. Whereas the qL-pulses superpose well into a smooth normal surface, the qT-mode arrivals cannot be simply detected. To better understand this phenomenon, a numerical simulation was performed. For the material properties known from results of a classical PS/PR technique [12], synthetically evaluated fields of a linear array of point-like sources were superposed, resulting in Fig. 3c. Similarly to the experiment, the qL-wavefronts superposed into a new wavefront, with a shape similar to synthetic pulses from particular sources. The superposed qT-field exhibits the same disorder as observed in the experiment.

Explanation should be sought in energy focusing on the qT ray surface. Besides the superposed planar wave, the detector receives wave arrivals from particular sources. Due to the energy focusing especially on the edges of cuspidal regions, these waves can be of considerably higher amplitudes than the whole superposed planar wave. Moreover, the velocities corresponding to the edges of the cuspidal regions are usually global maxima of the whole qT ray surface, thus arriving sooner than the planar wave. When uniform energy distribution along the ray surfaces is considered (Fig. 3d), a significant superposed qT-wavefront arises. As proven by other simulations, neither further densification (resolution increase) nor arbitrary elongation of the array can weaken this effect of energy focusing – i.e., the response to a large number of point-like loadings does not converge to a response to a line source. The only possible improvement comes from decreasing the step in the angles β, both in the calculation and experiment. Then, the superposed wavefronts form smooth normal surfaces, whereas the particular arrivals in energetically-preferred directions should appear as solitary localized maxima (see Fig. 4) However, decreasing the angular step in β is disadvantageous due to the large number of measurements required.

4. Application to general arrays

Let us now return to determination of phase velocities via the extremal condition (2). To obtain sufficiently smooth $[y, t]$-fields for a reasonable number of angles β, the same problem of the large number of required measure-

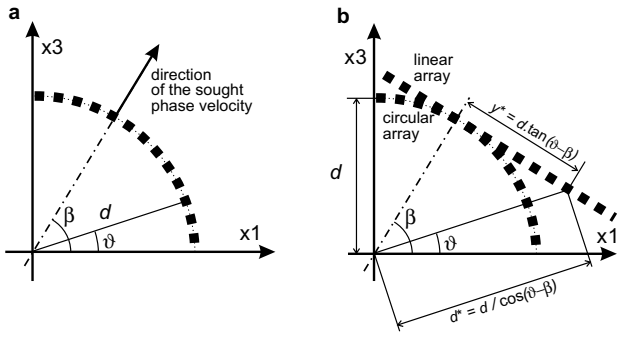

Fig. 5. A polar PS/PR scan with a constant radius d and angular step $\Delta\vartheta$ (a) and construction of the corresponding linear array for each angle β (b).

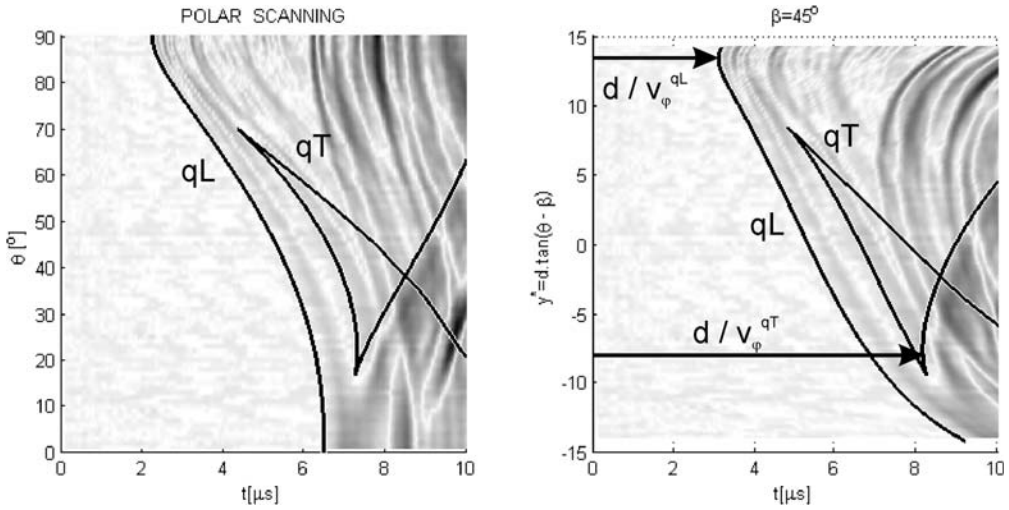

Fig. 6. Results of a polar PS/PR scan and its transformation into a $[y^*, t]$-field for determination of the phase velocity in direction $\beta = 45°$. The polar scan was performed for a 8 mm thick plate of a unidirectional CFRP composite with the fibre direction parallel to the x_3-axis by scanning a quarter of a circle of diameter $d = 20$ mm by an angular step of $\Delta\vartheta = 1°$. Thick lines denote the arrivals of particular wavefronts evaluated for known elastic coefficients.

ments arises. However, the findings from the first section can be utilized for circular or arbitrary curved arrays of point-like sources.

Let us consider a set of signals obtained from a polar PS/PR scan. With a detector considered in the origin of the cartesian system again, the geometry is outlined in Fig. 5a. The angular coordinate ϑ denotes the position of a particular source, scanning the arc of a constant radius d, angularly spaced by $\Delta\vartheta$, where ϑ is the angle which join on the actual source and the detector forms with the x_1-axis.

Our aim is now to determine the phase velocity for any given angle β. The wavefronts of particular modes arrive on the detector in times

$$\mathrm{TOF}(\vartheta) = \frac{d}{v_{\mathrm{G}}(\vartheta)}. \tag{6}$$

If the array was linear and forming the angle β with the x_3-axis, the distance of the source corresponding to direction ϑ would be $d^* = d/\cos(\vartheta - \beta)$, see Fig. 5b for clarity. And, consequently, the times of flight (TOFs) would transform into

$$\mathrm{TOF}^*(\vartheta) = \frac{d^*}{v_{\mathrm{G}}(\vartheta)} = \frac{d}{v_{\mathrm{G}}(\vartheta)\cdot\cos(\vartheta - \beta)}. \tag{7}$$

This function has the same properties as (1), reaching, analogically, its minimum in

$$\min_{\vartheta\in\langle 0°,90°\rangle} \mathrm{TOF}^* = \mathrm{TOF}^*(\vartheta_0) = \frac{d}{v_{\mathrm{G}}(\vartheta_0)\cdot\cos(\vartheta_0 - \beta)} = \frac{d}{v_\varphi(\beta)}. \tag{8}$$

By the transformation $\mathrm{TOF} \to \mathrm{TOF}^*$ we are treating the sources of the circular array as if they were arranged in a line. An example of resultant field is presented in Fig. 6. For $\beta = 45°$, we obtain a field similar to that in Fig. 1, only with the y-axis scaled by

$$y^* = d\cdot\tan(\vartheta - \beta). \tag{9}$$

The phase velocities in chosen direction β can be, again, directly determined from the minima of the TOFs.

5. Concluding remarks

All of the above described approaches enable the phase velocities of acoustic waves in anisotropic solids to be detected in chosen directions. The superposition approach offers the most direct method of phase velocity determination. However, it was shown that this approach is inapplicable to wavefronts with significant energy focusing. Surprisingly, increasing the resolution of the linear array does not induce a convergence of the superposed field to a response to a line source.

The presented methods are most suitable for the fastest qL-mode, which might be completely insufficient for stable determination of elastic coefficients [16,17]. For the qT-modes, where considerable energy focusing usually appears, the methods based on the extremal condition (2) can be, with some limitations, applied, whereas the superposition approach fails. It must be mentioned that the proposed approaches, except the superposition again, enable an analytical phase velocity error estimation. For the $[y, t]$-field obtained from a linear array, let α_0 be the point where the minimal TOF is reached. So, we take $v_\varphi(\beta) = \frac{d}{\mathrm{TOF}(\alpha_0)}$ with a variance

$$\sigma^2_{v_\varphi(\beta)} = \left(\frac{1}{\mathrm{TOF}(\alpha_0)}\right)^2\sigma_d^2 + \left(\frac{d}{\mathrm{TOF}^2(\alpha_0)}\underbrace{\left.\frac{\mathrm{dTOF}(\alpha)}{\mathrm{d}\alpha}\right|_{\alpha=\alpha_0}}_{\approx 0}\right)^2\sigma_\alpha^2, \tag{10}$$

concluding that for $\Delta y \ll d$, the accuracy of v_φ is given mainly by the accuracy of the distance d. For the conventional geo-

metrical conversion, such error estimation is impossible, and the effect of conversion on the resultant accuracy must be determined from Monte Carlo simulations [11].

The presented methods, as well as conventional PS/PR techniques, are limited to the symmetry planes. This limitation may be crucial for single crystals or biological materials, but it is irrelevant to composites. Similarly, all the problems known from the classical PS/PR techniques, such as unreliable identification of low-energy branches of the qT-mode, can be expected to appear in above described approaches. However, the advantage of avoiding the geometrical conversion from phase to group velocities makes the approaches presented simpler, more stable, and more suitable for automation.

Acknowledgements

This work was supported by the Grant Agency of the Academy of Sciences of the Czech Republic under Project No. IBS2076356. The authors also like to express their thanks to Mr. C. O'Neill for correcting the manuscript, and to Dr. P. Šittner for helpful comments.

References

[1] A.G. Every, W. Sachse (Eds.), Dynamic Methods for Measuring the Elastic Properties of Solids, Handbook of Elastic Properties of Solids, Liquids and Gases, 1, Academic Press, San Diego, 2001;
A.G. Every, W. Sachse, NDT&E Int. 29 (1996) 225–236.
[2] A.G. Every, W. Sachse, Phys. Rev. B 42 (1990) 8196–8205.
[3] W. Sachse, K.Y. Kim, N.N. Hsu, in: A. Wirgin (Ed.), Identification of media and structures by inversion of mechanical wave propagation, CISM Proc. Udine 1998 vol. 67 (1990) 2753–2761.
[4] K.Y. Kim, W. Sachse, Phys. Rev. B 47 (1993) 10993–11000.
[5] K.Y. Kim, R. Sribar, W. Sachse, J. Appl. Phys. 77 (1995) 5589–5600.
[6] B. Audoin, C. Bescond, M. Deschamps, J. Appl. Phys. 80 (1996) 3760–3771.
[7] B. Audoin, Ultrasonics 40 (2002) 736–740.
[8] H. Seiner, M. Landa, in: M.Černý (Ed.), International Symposium on Mechanics of Composites, Prague, 2002, pp. 129–136.
[9] H. Seiner, M. Landa, Acta Technol., CSAV 47 (2002) 400–418.
[10] H. Seiner, M. Landa, in: C. Pappalettere (Ed.), Proceedings of ICEM12 – 12th International Conference on Experimental Mechanics, Bari, 2004, on CD-ROM.
[11] H. Seiner, M. Landa, Ultrasonics 43 (2005) 253–263.
[12] H. Seiner, Master's Thesis, Czech Technical University in Prague, 2004.
[13] B.A. Auld, Acoustic Fields and Waves Solids, vol. 1, John Wiley and Sons, New York, 1973.
[14] M.J.P. Musgrave, Crystal Acoustics, Holden-Day, San Francisco, 1970.
[15] R.F.S. Hearmon, Introduction to Applied Anisotropic Elasticity, Oxford University Press, 1961, 1992, pp.567–573.
[16] A.G. Every, W. Sachse, Ultrasonics 30 (1992) 43–48.
[17] Y.C. Chu, S.I. Rokhlin, J. Acoust. Soc. Am 95 (1994) 213–225.